

Light Scattering Spectra of Water in Trehalose Aqueous Solutions: Evidence for Two Different Solvent Relaxation Processes

M. Paolantoni,^{*,†} L. Comez,^{‡,§} M. E. Gallina,[†] P. Sassi,[†] F. Scarponi,[‡] D. Fioretto,[‡] and A. Morresi[†]

Dipartimento di Chimica, Università di Perugia, Via Elce di Sotto, 8, I-06123 Perugia, Italy, CNISM-Dipartimento di Fisica, Università di Perugia, Via Pascoli, I-06123 Perugia, Italy, and CRS SOFT INFN-CNR, c/o Dipartimento di Fisica, Università La Sapienza, P.le Aldo Moro 4, I-00185 Roma, Italy

Received: January 17, 2009; Revised Manuscript Received: March 30, 2009

Light scattering spectra on aqueous solutions of trehalose were recorded in a wide frequency range combining the use of a double monochromator and a multipass Fabry–Perot interferometer. Experimental results indicate the presence of a slow relaxation mode related to the solute dynamics, which is clearly separated from the solvent one. The spectral analysis reveals the existence of two separate solvent relaxation processes assigned to hydrating and bulk water molecules. The picosecond dynamics of water molecules directly interacting with the solute (proximal water) is consistently delayed with the corresponding relaxation time increase is about 5–6 times compared to the bulk. The slowing down induced by the sugar on the water dynamics mainly involves a restricted hydration layer constituted of 16–18 water molecules. These results improve our knowledge about the influence of carbohydrates on the fast rearrangement dynamics of water and may serve as a model to gain important insight on basic solvation properties of other biorelevant systems in aqueous media.

I. Introduction

Structural and dynamical properties of water play a major role in several chemical and biological processes. In the presence of solutes, the aqueous solvent cannot be represented considering a unique picture: important differences on relevant relaxation properties existing between bulk and hydration water were pointed out. The dynamical characterization of solvating water constitutes a crucial subject of investigation.^{1–4}

In the case of biological molecules, such as proteins and DNA, the study of water localized in proximity of the biomolecule, sometime referred to as biological water, is essential for the comprehension of many biological processes.³ Recent works indicated that the dynamics of the biological water is substantially retarded with respect to the bulk.^{3,4} However, direct experimental evidence of the presence of different dynamical regimes of water in aqueous solutions is very difficult to attain, especially in the case of small solutes with inherent relaxation contributions at similar temporal scales of the solvent ones.

Aqueous solutions of simple carbohydrates represent a convenient model to achieve a deep understanding of fundamental hydration properties which may also occur in more complex biological systems. Carbohydrates are themselves interesting due to the role they play in different biological processes and are subjected to intense investigations owing to their bioconservative capabilities.^{5,6} In particular, the disaccharide trehalose shows an exceptional effectiveness in preserving the structure and the function of several biomolecules.^{6–11} A recent study shows that trehalose is implicated in the intracellular glass formation and that cell membranes were protected by replacement of water by the sugar.¹² The detailed molecular

origin of these conservative properties is still under study; thus, understanding the specific role played by water–sugar interactions and the fundamental properties of the sugar hydration deserve careful investigation. In this context, the study of the water relaxation dynamics at picosecond time scales in carbohydrate solutions represents an important first step in order to clarify the whole phenomenon.

From an experimental point of view, the characterization of the dynamics of hydration water in this kind of systems is challenging mainly for two reasons. First, the different dynamical processes, which may include solute and solvent relaxation modes, generally cover wide frequency ranges, which cannot be completely explored with a single spectroscopic technique. Second, hydration water can be distinguished from bulk water as long as the observed relaxation process is faster than their reciprocal exchange (slow exchange conditions); otherwise only a single average spectrum that accounts for the two contributions is obtained. Here, we show that depolarized light scattering experiments are suitable tools for the investigation of the fast relaxation dynamics of water in sugar solutions.

Previous experiments have focused on the hydration properties of trehalose analyzing different spectral ranges. Ultrasonic experiments on trehalose–water solutions, performed in the megahertz frequency region, indicated a solute hydration number of about 9–15,¹³ which is in agreement with the results derived by viscosity measurements.¹⁴ The whole picture was confirmed by quasi-elastic neutron scattering experiments in the 8–800 GHz frequency range.¹⁵ Concerning the dynamics of hydration water, significant information was provided by molecular dynamics simulations.¹⁶ In this respect, Lee et al. investigated sugar hydration properties characterizing relevant relaxation processes in the 0.1–20 ps temporal range;¹⁶ these studies demonstrated that the water translational and rotational mobility strongly depends on the distance from the sugar molecule and that the dynamical delay generally occurs within about 5.5 Å

* To whom correspondence should be addressed. E-mail: marcopa@unipg.it.

[†] Dipartimento di Chimica, Università di Perugia.

[‡] CNISM-Dipartimento di Fisica, Università di Perugia.

[§] Università La Sapienza.

from the solute. The retardation effect was primarily attributed to the formation of stable carbohydrate–water hydrogen bonds and for trehalose an average hydration number of 13.5 was obtained at 30 °C. Subsequently, terahertz (THz) spectroscopy experiments^{17,18} revealed the strong influence of the sugar on the water absorption coefficient and suggested that the perturbation of the solute extends beyond the first solvation shell. This led to the definition of an expanded dynamical hydration shell that encompasses a greater number of water molecules than reported before.^{13–15} Thus, even for relatively simple solutes descriptions of hydration shell and hydration number are not univocal being dependent on the characteristic time scale of the experiment. In this scenario, it is essential to compare results coming from different techniques in order to achieve a full comprehension of hydration properties.

In this work, we give the direct experimental evidence of the existence of different dynamical regimes of water in trehalose aqueous solutions by means of depolarized light scattering investigations performed in a very wide frequency range. The imaginary part of the dynamical susceptibility is obtained in the range from 0.3 GHz to 30 THz, splicing the spectra recorded using a double monochromator and a multipass Fabry–Perot interferometer.^{19,20} The rotational diffusion of trehalose can be properly separated from the relaxation process of water, taking advantage of the weak overlap of the corresponding spectral features. As a result, the spectral region related to the water dynamics was conveniently analyzed and the presence of two distinct relaxation modes related to bulk and hydration water was unambiguously proven. Moreover, the perturbation of the relaxation dynamics of hydrating water caused by the solute was experimentally quantified.

II. Experimental Section

D-(+)-Trehalose dehydrate was purchased from Fluka Sigma-Aldrich with purities higher than 99.5%. Doubly distilled and deionized water was prepared in our laboratory. The solutions were prepared by weight, adding the sugar to water then stirring and heating them until the solute was completely dissolved. All the solutions were freshly prepared and conditioned for more than one hour before measurements. Moreover, in order to avoid scattering from dust particles, they were purified through a cellulose 0.22- μ m Millipore filter. All the samples were placed in a 10 mm path quartz cuvette.

Depolarized light scattering (DLS) measurements were performed on trehalose–water solutions at different molar fractions x_T , ($0 \leq x_T \leq 0.031$) and $T = 35$ °C using the experimental setup described in refs 19 and 20. A Coherent-Innova Ar⁺ laser operating on a single mode at $\lambda_0 = 514.5$ nm was used as light source (typical power of ~ 500 mW) and the horizontally polarized scattered light was analyzed by means of two different spectrometers.

The low-frequency region from 0.01 to 7 cm^{-1} (0.3–200 GHz) was recorded, by means of a Sandercock-type (3 + 3)-pass tandem Fabry–Perot interferometer, characterized by a finesse of about 100 and a contrast $> 5 + 10^{10}$. Three different mirror separations, $d = 14$ –15 mm, $d = 4$ –4.5 mm and $d = 1$ –1.5 mm, corresponding to distinct free spectral ranges, were used. The backscattering geometry was employed in order to avoid intense contributions to the spectra coming from transverse acoustic modes. The cuvette containing the samples was placed in a thermo-controlled copper holder; the heating was realized by a conventional dc power supply and temperature fluctuations were kept within 0.1 °C during the spectra recording.

Higher frequency measurements were recorded in the 1–1200 cm^{-1} frequency range using an ISA Jobin-Yvon model U1000

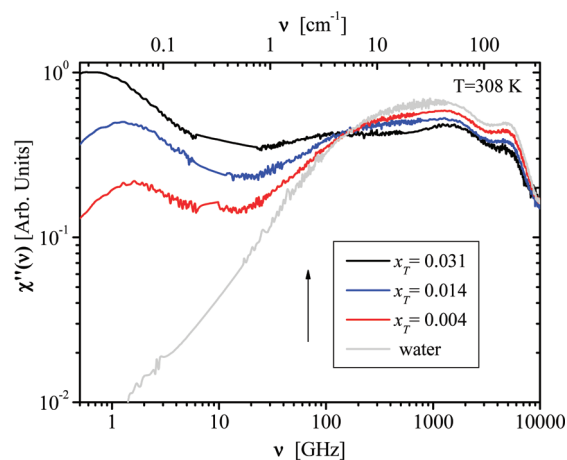


Figure 1. Imaginary part of the susceptibility of pure water and trehalose/water solutions at different sugar molar fractions. The arrow indicates the direction of a concentration increase. Depicted spectra were normalized referring to the amplitude of the water relaxation modes as derived by the employed fitting procedure (see text for details). The connecting line around 10 GHz substitutes few spurious points originated by the leakage of the Brillouin peaks.

double monochromator having 1 m focal length with holographic gratings. The scattered light was collected using a thermoelectrically cooled Hamamatsu model 943XX photomultiplier that is computer-controlled by the ISA Jobin-Yvon SpectraMax package adopting a 90° scattering geometry. The spectra were recorded in two different frequency regions: from -10 to 10 cm^{-1} with a resolution of 0.5 cm^{-1} and from 5 to 1200 cm^{-1} with a resolution of 2 cm^{-1} . The temperature was controlled by circulating water from a Haake F6 ultrathermostat with a precision of 0.1 °C.

After subtraction of the dark count contribution, low- and high-frequency spectra were spliced taking advantage of an overlap of about half a decade in frequency. Further, the susceptibility spectra were calculated as the ratio between the $I_{\text{VH}}(\nu)$ intensity and $[n(\nu)+1]$, where $n(\nu)$ is the Bose–Einstein occupation number, namely $n(\nu) = [\exp(\beta) - 1]^{-1}$ with $\beta = h\nu/kT$.^{19,20}

III. Results and Discussion

Representative susceptibility spectral distributions are reported in Figure 1. The lower frequency peak, below 10 GHz, is assigned, in analogy with a previous work,¹⁹ to the trehalose rotational diffusion: this relaxation mode is absent in pure water and its intensity increases with the sugar concentration. The highest frequency region (10^3 – 10^4 GHz) is assigned to the intermolecular bending and stretching resonant modes of water molecules;^{19–22} while the intermediate spectral distribution, which extends from 10 to 10^3 GHz, is related to the characteristic relaxation process of water.^{19,20,23,24} The relative intensity decrease observed in the 10^2 – 10^4 GHz region with increasing the sugar concentration and its modeling (see below) in terms of the pure water functional forms indicate that sugars lead to minor direct contributions; this supports previous interpretations.^{19–22} The rotational relaxation contribution of trehalose can be properly reproduced by means of a Cole–Davidson functional form. The corresponding average relaxation time increases with the trehalose concentration from about 130 to 350 ps. The analysis of this mode is not the object of the present work and will be examined in details in a forthcoming study.

The small interference between solute and solvent bands, which appear at very different frequency regions, allows the

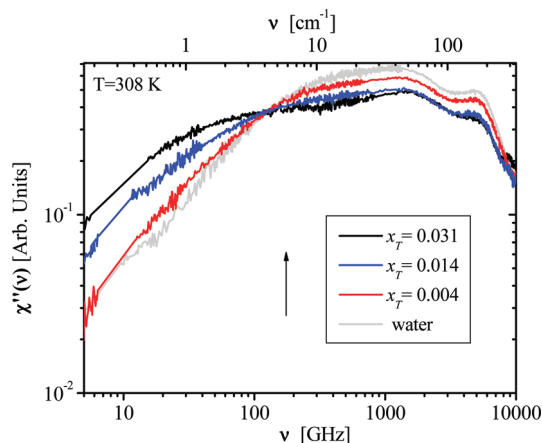


Figure 2. Imaginary part of the susceptibility of pure water and trehalose/water solutions at different sugar molar fractions after subtraction of the low-frequency sugar contribution. The arrow indicates the direction of a concentration increase.

subtraction of the trehalose signal from the total spectrum to completely isolate the water contribution. The resulting spectra related to the intermolecular and to the relaxation dynamics of water are reported in Figure 2. Concerning the spectral region due to the water relaxation dynamics, it can be observed that the intensity decreases at around 500 GHz, while a new contribution grows up around 30 GHz by increasing the sugar concentration. A quasi-isosbestic point may be detected at ca. 200 GHz. As will be illustrated below, this behavior can be interpreted considering the presence of two distinct spectral contributions ascribed to water molecules transiently localized in different environments. Upon trehalose addition, the higher frequency component, also present in neat water, is partially replaced by a lower frequency one related to a slower relaxation process. It is worth noting that in relation to the picosecond relaxation dynamics of water within solutions of simple solutes, to our knowledge this constitutes the first direct experimental evidence of the presence of two distinct spectral contributions.

In order to achieve quantitative information from the spectral distribution, a fitting procedure was applied. After the subtraction of the low-frequency sugar contribution, the susceptibility $\chi''(\omega)$ was modeled as the sum of four contributions: two Cole-Davidson (CD) functions to reproduce the water relaxation modes and two damped harmonic oscillator (DHO) functions for the resonances at 60 and 170 cm^{-1} related to the intermolecular bending and stretching modes of water molecules, respectively

$$\chi''(\omega) = \mathcal{Im} \left\{ -\frac{\Delta_{\text{slow}}}{[1 + i\omega\tau_{\text{slow}}]^{\beta_{\text{slow}}}} - \frac{\Delta_{\text{fast}}}{[1 + i\omega\tau_{\text{fast}}]^{\beta_{\text{fast}}}} + \frac{\Delta_b\omega_b^2}{\omega^2 - \omega_b^2 - i\omega\Gamma_b} + \frac{\Delta_s\omega_s^2}{\omega^2 - \omega_s^2 - i\omega\Gamma_s} \right\}$$

where Δ is the relative amplitude of each term, τ_{slow} , β_{slow} and τ_{fast} , β_{fast} are the characteristic times and stretching parameters of the two water relaxation terms, respectively; ω_b , ω_s , Γ_b , Γ_s are the characteristic frequencies and widths of the intermolecular bending and stretching modes of water, respectively. The use of the two DHO functions is in agreement with previous investigations^{22,24} while the choice of a Cole–Davidson function for the relaxation terms is consistent with recent studies where a nonexponential behavior for the water relaxation process is considered.^{23,25,26} After checking that the results of the fitting

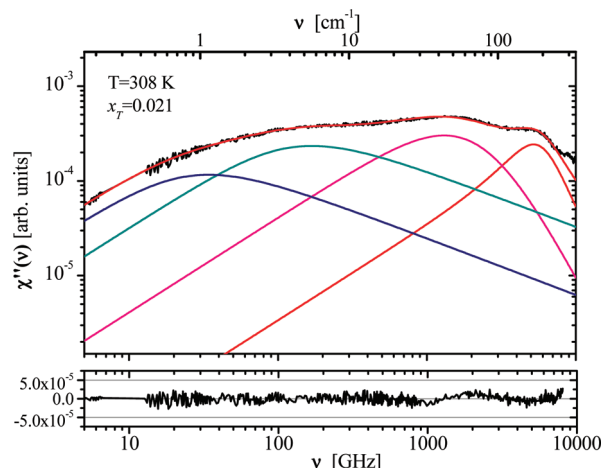


Figure 3. Imaginary part of the susceptibility of a trehalose/water solution, $x_T = 0.021$, after subtraction of the sugar contribution. Experimental data (black line) are shown together with the total fitting curve (red line) and the different components: slow water relaxation mode (blue line), fast water relaxation mode (green line), water bending (purple line), and stretching (orange line) resonant modes. The panel below depicts the difference between the best-fit result and the experimental curve.

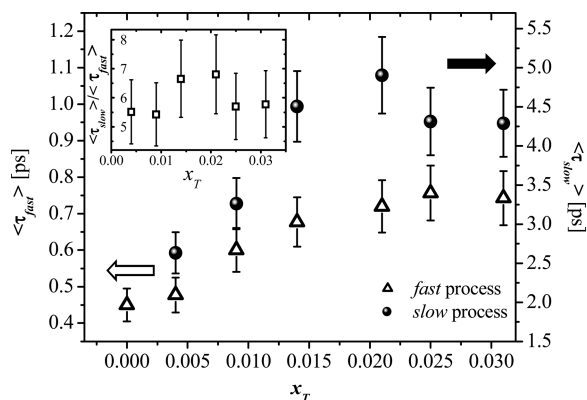


Figure 4. The slow (spheres) and fast (triangles) average relaxation times of the two water relaxation processes as a function of the trehalose molar fractions x_T as obtained by the employed fitting procedure. In the inset, the relative increment between the two relaxation times is reported as a function of x_T .

procedure do not strongly depend on the stretching parameters, we fixed their values at 0.6, as obtained in pure water,²⁰ to reduce the number of free fitting parameters. Figure 3 shows a typical best-fit result obtained for a trehalose–water solution of an intermediate concentration. We remark that any attempt to reproduce the experimental profiles using a single relaxation term was unsuccessful and that the use of a new low-frequency component was necessary to correctly model the spectral portion below 200 GHz.

The average relaxation time $\langle\tau\rangle = \tau\beta$ of the two water contributions obtained at different sugar concentrations is reported in Figure 4. The fast process, also present in neat water, shows a characteristic average relaxation time in the 0.4–0.8 ps range, while the slow process has a characteristic time constant of about 3–4 ps. Both relaxation times slightly increase with increasing trehalose concentration. The fast relaxation, also present in neat water, can be assigned to the solvent molecules scarcely influenced by the solute. On a molecular basis, this process accounts for the fast rearrangement of local structures (transient cages).^{20,21,26} In this case the modulation of the system's polarizability anisotropy, the

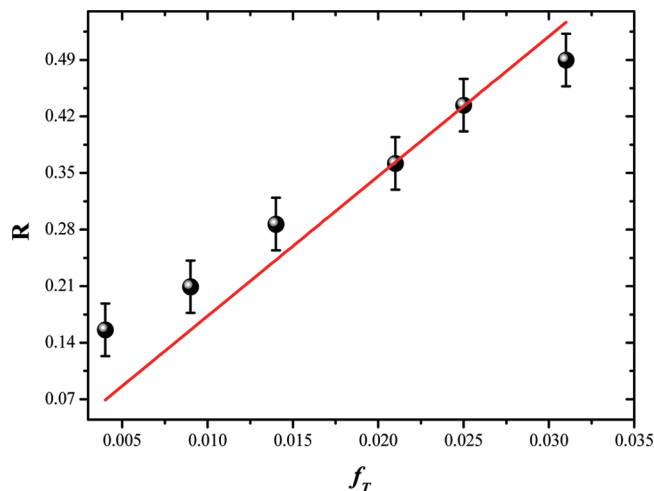


Figure 5. The relative weight $R = \Delta_{\text{slow}}/(\Delta_{\text{slow}} + \Delta_{\text{fast}})$ of the slow water relaxation process as a function of the trehalose molar ratio f_T . Quoted error bars refer to statistical inaccuracies resulting by the fitting procedure. The line represents the best-fit result of a linear regression with intercept value constrained to zero as required by the adopted model (i.e., $R = N_H f_T$). An average hydration number N_H of 17 ± 1 is obtained.

relevant physical quantity in both DLS and time-resolved optical Kerr effect experiments, is mainly related to intermolecular (collision-induced) contributions.^{20,21,26} The corresponding relaxation time is often regarded as a measure of the average hydrogen bond lifetime in water.^{20,21,27} The slower process detected can then be ascribed to the corresponding relaxation dynamics of water molecules more strongly perturbed by the presence of the sugar (hydration water). The dynamical slowing down may be explained considering the formation of stable sugar–water hydrogen bonds.¹⁶ In this sense τ_{slow} describes a local restructuring process which essentially involves the inner hydration layer of the solute also referred to as static hydration shell.¹⁸ It is worthy of note that τ_{slow} also represents a lower limit value of the water residence time in this static hydration shell; in other words to allow the detection of two distinct spectral contributions the average time required for the exchange of water molecules between the hydration shell and the bulk must be long compared to τ_{slow} . This situation is consistent with experimental and computational studies on hydration shells of simple ions, which assign at tens of picoseconds the characteristic residence times of water.^{1,2,28,29}

Besides dynamical information, depolarized light scattering spectra were also employed to estimate the average hydration number N_H , which is the average number of water molecules localized in the sugar hydration layer. In our case N_H is defined as the number of water molecules transiently localized in the hydration layer of the sugar molecules (and that contribute to the intensity of the slow relaxation term) divided by the total number of sugar molecules in solution. Thus, the ratio R between the amplitude of the slow process and that of the total water contribution (bulk and hydrating water) to the relaxation, $R = \Delta_{\text{slow}}/(\Delta_{\text{slow}} + \Delta_{\text{fast}})$, can be related to N_H by the following relationship: $R = N_H f_T$, where f_T is the trehalose/water molar ratio. Figure 5 shows R versus f_T together with the corresponding linear fit performed constraining the intercept value to the origin. The observed linear correlation reasonably confirms the proposed model; the larger deviations observed at lower concentrations may be due to larger inaccuracies related to the small intensity contribution of the slow component. This

analysis leads to a hydration number $N_H = 17 \pm 1$. The average number of trehalose–water hydrogen bonds calculated in simulation studies is 12–14,^{16,18} which is in agreement with ultrasonic, viscosity, and quasi-elastic neutron scattering experiments.^{13–15} This supports the idea that the slow relaxation process can be essentially ascribed to water molecules more directly influenced by the solute due to the formation of trehalose–water hydrogen bonds. Our findings are also consistent with molecular dynamics simulation studies of trehalose aqueous solutions at different concentrations.^{30,31} In this case, the authors remarked that sugar–sugar interactions became relevant only at higher sugar contents, stating from $x_T = 0.048$. We find also useful to remark that the average N_H hydration number detected compares with the hydration number obtained in the simulation of Lebret et al.³¹ when a geometrical definition of hydrogen bond (criterion II³¹), which considers oxygen–oxygen distances less than 3.4 Å and O–H...O angles larger than 120°, is adopted, as also done in ref 16.

As a whole our results give evidence of the presence of an inner shell constituted of about 16–18 hydrating molecules per trehalose molecule with a dynamics retarded 5–6 times with respect to bulk water (see inset of Figure 4). The sugar-induced retardation on the water dynamics and the subsequent appearance of two different dynamical domains recall the findings derived by molecular dynamics simulations study of Lee et al.¹⁶ In this case structural and dynamical properties of proximal and bulk water were distinguished and numerically characterized; both translational and rotational dynamics were found to slow down in the vicinity of the carbohydrate. The relative increase between the rotational correlation time calculated for proximal (at sugar–water distances minor of ca. 3 Å) and bulk water molecules was about 2–4.¹⁶ The agreement with our data is rather remarkable also considering the different nature of the measured and computed relaxation times.

Light scattering experiments, depending on the anisotropy polarization of the medium, are proven to be a favorable tool to separate relaxation processes of solute and solvent in aqueous solutions. Conversely, two distinct contributions are not distinguishable using other spectroscopic techniques that essentially probe orientational relaxation dynamics. In dielectric spectra on sugar–water solutions, for example, only a single broad relaxation signal can be revealed.³² This may be explained recalling that dielectric spectroscopy is more sensitive to the reorientation of OH groups, rather than to that of the whole molecule; in addition, since the dipolar relaxation of water is typically located in the tens gigahertz relaxation region,²⁴ the slow exchange picture breakdowns.

Recent terahertz spectroscopy experiments have explored the dynamical hydration shell of carbohydrate^{17,18} and protein³³ aqueous solutions. In both systems, the thickness of the hydration layers was obtained taking into account the absorption coefficient enhancement caused by the solute on the water molecules. These experiments evidenced a long-range influence of carbohydrates on the surrounding water molecules which extends beyond the first hydration shell involving even more than one hundred water molecules.^{17,18} Although terahertz spectroscopy, probing frequency components related to dipolar relaxation at subpicosecond time scales, is probably more sensitive to minor dynamical variations related to ultrafast molecular motions, our DLS results indicate that the dominant retardation effect mainly concerns a more restricted number of water molecules. For these hydrating water molecules the perturbation extent can be evaluated by DLS experiments.

Finally, for the sake of comparison we briefly discuss previous DLS results obtained for glucose aqueous solutions. In this case, only a single relaxation contribution entailing both bulk and hydration water was detected. Using a simple model for the concentration dependence of the water relaxation time and considering an hydration number of 8–10,¹⁶ it was estimated that the dynamics of proximal water slows down by a factor of about three.^{20,21} In the present study, we take advantage of the slower sugar dynamics which permits a more detailed analysis of the water relaxation region. Moreover, even if the different modeling prevents from a quantitative comparison, experimental features evidence that the disaccharide not only influences the dynamics of a larger number of water molecules compared to the monosaccharide, but also causes a more sensitive slowing down of the relaxation of proximal water. This tendency is in qualitative agreement with molecular dynamics simulation studies where different sugars were examined.^{16,18,30,31}

IV. Conclusions

The use of two different experimental setups (a dispersive and an interferometric equipments) allowed us the analysis of a very large frequency domain that includes the relaxation mode of the solute and both relaxation and resonant modes of the aqueous medium. Referring to the first hydration layer of the solute, unambiguous evidence of the considerable slowing down of the water relaxation process was demonstrated isolating spectral features due to bulk and hydration water contributions. Notably, the retardation effect induced by carbohydrates on the water dynamics may be related to the bioconservative properties of this class of compounds.^{6,18} In the present work, we demonstrated that the solute strongly affects the fast relaxation dynamics at picosecond time scales, moreover, the extent of this effect was experimentally quantified. The rearrangement dynamics of hydrating water was found 5–6 times slower than the bulk. Each trehalose molecule mainly restricts the relaxation dynamics of ca. 16–18 water molecules which essentially represent the solvent molecules hydrogen bonded with the solute. Overall results may constitute useful starting point for the understanding of basic hydration properties of more complex biologically relevant macromolecules.

References and Notes

- (1) Kropman, M. F.; Bakker, H. J. *Science* **2001**, 291, 2118.
- (2) Kropman, M. F.; Nienhuys, H.-K.; Bakker, H. J. *Phys. Rev. Lett.* **2002**, 88, 077601.
- (3) Pal, S. K.; Peon, J.; Zewail, A. H. *Proc. Natl. Acad. Sci. U.S.A.* **2002**, 99, 1763.
- (4) Bagchi, B. *Chem. Rev.* **2005**, 105, 3197.
- (5) O'Connor, T. F.; Debenedetti, P. G.; Carbeck, J. D. *J. Am. Chem. Soc.* **2004**, 126, 11794.
- (6) Magazù, S.; Migliardo, F.; Telling, M. T. F. *Eur. Biophys. J.* **2007**, 36, 163.
- (7) Crowe, J. H.; Crowe, L. M.; Chapman, D. *Science* **1984**, 223, 701.
- (8) Wright, J. C.; Westh, P.; Ramlov, H. *Biol. Rev.* **1992**, 67, 1.
- (9) Carpeneter, J. F.; Prestrelski, S. J.; Arakawa, T. *Arch. Biochem. Biophys.* **1993**, 303, 456.
- (10) Sola-Penna, M.; Meyer-Fernandes, J. R. *Arch. Biochem. Biophys.* **1998**, 360, 10.
- (11) Cesàro, A. *Nat. Mater.* **2006**, 5, 593.
- (12) Sakurai, M.; Furuki, T.; Akao, K.; Tanaka, D.; Nakahara, Y.; Kikawada, T.; Watanabe, M.; Okuda, T. *Proc. Natl. Acad. Sci. U.S.A.* **2008**, 105, 5093.
- (13) Magazù, S.; Migliardo, P.; Musolino, A. M.; Sciortino, M. T. *J. Phys. Chem. B* **1997**, 101, 2348.
- (14) Branca, C.; Magazù, S.; Maisano, G.; Migliardo, F.; Migliardo, P.; Romeo, G. *J. Phys. Chem. B* **2001**, 105, 10140.
- (15) Magazù, S.; Villari, V.; Migliardo, P.; Maisano, G.; Telling, M. T. F. *J. Phys. Chem. B* **2001**, 105, 1851.
- (16) Lee, S. L.; Debenedetti, P. G.; Errington, J. R. *J. Chem. Phys.* **2005**, 122, 204511.
- (17) Heugen, U.; Schwaab, G.; Bründermann, E.; Heyden, M.; Yu, X.; Leitner, D. M.; Havenith, M. *Proc. Natl. Acad. Sci. U.S.A.* **2006**, 103, 12301.
- (18) Heyden, M.; Bründermann, E.; Heugen, U.; Niehues, G.; Leitner, D. M.; Havenith, M. *J. Am. Chem. Soc.* **2008**, 130, 5773.
- (19) Fioretto, D.; Comez, L.; Gallina, M. E.; Morresi, A.; Palmieri, L.; Paolantoni, M.; Sassi, P.; Scarponi, F. *Chem. Phys. Lett.* **2007**, 441, 232.
- (20) Paolantoni, M.; Comez, L.; Fioretto, D.; Gallina, M. E.; Morresi, A.; Sassi, P.; Scarponi, F. *J. Raman Spectrosc.* **2008**, 39, 238.
- (21) Paolantoni, M.; Sassi, P.; Morresi, A.; Santini, S. *J. Chem. Phys.* **2007**, 127, 024504.
- (22) Wang, Y.; Tominaga, Y. *J. Chem. Phys.* **1994**, 100, 2407.
- (23) Sokolov, A. P.; Hurst, J.; Quitmann, D. *Phys. Rev. B* **1995**, 51, 12865.
- (24) Fukasawa, T.; Sato, T.; Watanabe, J.; Hama, Y.; Kunz, W.; Buchner, R. *Phys. Rev. Lett.* **2005**, 95, 197802.
- (25) Santucci, S. C.; Fioretto, D.; Comez, L.; Gessini, A.; Masciovecchio, C. *Phys. Rev. Lett.* **2006**, 97, 225701.
- (26) Torre, R.; Bartolini, P.; Righini, R. *Nature* **2004**, 428, 296.
- (27) Teixeira, J.; Luzar, A.; Longeville, S. *J. Phys.: Condens. Matter* **2006**, 18, S2353.
- (28) Bakker, H. J.; Kropman, M. F.; Omta, W. J. *J. Phys.: Condens. Matter* **2005**, 17, S3215.
- (29) Chowdhuri, S.; Chandra, A. *J. Phys. Chem. B* **2006**, 110, 9674.
- (30) Bordat, P.; Lerbret, A.; Demaret, J.-P.; Affouard, F.; Descamps, M. *Europhys. Lett.* **2004**, 65, 41.
- (31) Lerbret, A.; Bordat, P.; Affouard, F.; Descamps, M.; Migliardo, F. *J. Phys. Chem. B* **2005**, 109, 11046.
- (32) Fuchs, K.; Kaatz, U. *J. Chem. Phys.* **2002**, 116, 7137.
- (33) Ebbinghaus, S.; Kim, S. J.; Heyden, M.; Yu, X.; Heugen, U.; Gruebele, M.; Leitner, D. M.; Havenith, M. *Proc. Natl. Acad. Sci. U.S.A.* **2007**, 104, 20749.

JP9004983